Remote Sens. **2015**, *7*, 1135-1153; doi:10.3390/rs70101135

OPEN ACCESS

remote sensing

ISSN 2072-4292

www.mdpi.com/journal/remotesensing

Article

The Thermal Infrared Sensor (TIRS) on Landsat 8: Design Overview and Pre-Launch Characterization

Dennis C. Reuter [1,*], Cathleen M. Richardson [2], Fernando A. Pellerano [3], James R. Irons [4], Richard G. Allen [5], Martha Anderson [6], Murzy D. Jhabvala [7], Allen W. Lunsford [8], Matthew Montanaro [9], Ramsey L. Smith [1], Zelalem Tesfaye [10] and Kurtis J. Thome [9]

1 NASA/GSFC, Code 693, Greenbelt, MD 20771, USA; E-Mail: Ramsey.L.Smith@nasa.gov
2 NASA/GSFC, Code 490, Greenbelt, MD 20771, USA; E-Mail: cathleen.m.richardson@nasa.gov
3 NASA/GSFC, Code 590, Greenbelt, MD 20771, USA; E-Mail: fernando.a.pellerano@nasa.gov
4 NASA/GSFC, Code 610, Greenbelt, MD 20771, USA; E-Mail: james.r.irons@nasa.gov
5 Kimberly Research and Extension Center, Kimberly, ID 83341, USA; E-Mail: rallen@kimberly.uidaho.edu
6 USDA Agricultural Research Service, Beltsville, MD 20705, USA; E-Mail: martha.anderson@ars.usda.gov
7 NASA/GSFC, Code 550, Greenbelt, MD 20771, USA; E-Mail: murzy.d.jhabvala@nasa.gov
8 NASA/GSFC/CUA, Code 693, Greenbelt, MD 20771, USA; E-Mail: allen.w.lunsford@nasa.gov
9 NASA/GSFC, Code 614, Greenbelt, MD 20771, USA; E-Mails: matthew.montanaro@nasa.gov (M.M.); kurtis.thome@nasa.gov (K.J.T.);
10 Millenium Engineering and Integration Company, Greenbelt, MD 20771, USA; E-Mail: zelalem.tesfaye@nasa.gov

* Author to whom correspondence should be addressed; E-Mail: dennis.c.reuter@nasa.gov; Tel.: +1-301-286-2042.

Academic Editors: Brian Markham and Prasad S. Thenkabail

Received: 21 August 2014 / Accepted: 15 December 2014 / Published: 19 January 2015

Abstract: The Thermal Infrared Sensor (TIRS) on Landsat 8 is the latest thermal sensor in that series of missions. Unlike the previous single-channel sensors, TIRS uses two channels to cover the 10–12.5 micron band. It is also a pushbroom imager; a departure from the previous whiskbroom approach. Nevertheless, the instrument requirements are defined such that data continuity is maintained. This paper describes the design of the

TIRS instrument, the results of pre-launch calibration measurements and shows an example of initial on-orbit science performance compared to Landsat 7.

Keywords: Landsat; LDCM; TIRS; thermal sensors; evapotranspiration; QWIP

Acronyms

Acronym	Definition
ASIC	Applications-specific integrated circuit
CCE	Cryocooler electronics
CDH	Command and data handling
DPAS	Data Processing and Archive System
EEPROM	Electrically-erasable, programmable, read-only memory
ERDAS	Earth Resources Data Analysis System
EROS	Earth Resources Observation and Science Center
ET	Evapotranspiration
ETM+	Enhanced Thematic Mapper+
FMEA	Failure mode effects analysis
FOV	Field of view
FPA	Focal plane assembly
FPE	Focal plane electronics
FPGA	Field-programmable gate arrays
GSFC	Goddard Space Flight Center
HEE	Half edge extent
HSI	High speed interface
IAS	Image Assessment System
IFOV	Instantaneous field of view
IRSM	Infrared source module
LDCM	Landsat Data Continuity Mission
MBE	Molecular beam epitaxy
MEB	Main electronics box
METRIC	Mapping EvapoTranspiration with high Resolution and Internalized Calibration
NEdL	Noise equivalent delta radiance
NEdT	Noise equivalent delta temperature
NIST	National Institute of Standards and Technology
NSLRSDA	National Satellite Land Remote Sensing Data Archive
OAP	Off-axis parabola
OLI	Operational Land Imager
PC	Printed circuit
QE	Quantum efficiency

QWIP	Quantum well infrared photodetector
RER	Relative edge response
ROIC	Read-out integrated circuit
RMS	Root mean square
SCA	Sensor chip assembly
SIDECAR	System for Image Digitization, Enhancement, Control and Retrieval
SRR	Systems Requirements Review
SSM	Scene select mechanism
TIRS	Thermal Infrared Sensor
TM	Thematic Mapper
TMU	Thermal-mechanical unit
USARL	U.S. Army Research Laboratory
USGS	United States Geological Survey
WRS2	Worldwide Reference System 2

1. Introduction

Landsat-8 (previously known as the Landsat Data Continuity Mission, LDCM), a joint NASA/USGS mission, was launched on 11 February 2013, with two instruments that are operated simultaneously, but independently: (1) the Operational Land Imager (OLI) that images in the visible, near-infrared and short-wave infrared; and (2) the Thermal Infrared Sensor (TIRS), a two-channel thermal imager. The goal of the LDCM was to continue the collection, archiving and distribution of multispectral imagery, affording global, synoptic and repetitive coverage of the Earth's land surfaces at a scale where natural and human-induced changes can be detected, differentiated, characterized and monitored over time. As the successor to the earlier Landsat satellites, the intent was to provide data into the future that is sufficiently consistent with previous Landsat data to allow the detection and quantitative characterization of land surface changes and to permit studies of land cover and land use change over multi-decadal periods. The data products are provided to the general public on a nondiscriminatory basis and at no cost to the users. The mission will provide Landsat data to the USGS National Satellite Land Remote Sensing Data Archive (NSLRSDA) at the USGS Earth Resources Observation and Science Center (EROS). This archive constitutes the longest continuous record of the Earth's surface as seen from space. In keeping with the Landsat continuity directive, the LDCM specifications, including ground resolution, swath width, radiometric and geometric accuracy and precision, and channel spectral bandwidths are compatible with the heritage Landsat specifications. It is important to note that, though thermal instruments have been on Landsat Mission satellites since Landsat 4, TIRS was not on the original manifest for LDCM. It was added quite late in the mission definition timeline, and as a result, the time from TIRS Systems Requirements Review (SRR) to when it was delivered to the spacecraft was only about three years. This is about one year shorter than a normal delivery schedule, and because of this, the TIRS schedule was always a significant driving force.

Both instruments introduced an operating concept new to the Landsat program, pushbroom sensor operation, in which rows of detectors for each channel are swept in the along-track direction by

spacecraft motion. For each channel, an image is built-up by concatenating successive single-row measurements. Previous Landsat instruments used whiskbroom operations, in which a few detectors for each channel are swept across track by a system of moving mirrors as the spacecraft travels in the along-track direction. Because, in a pushbroom sensor, each spatial element has its own detector, integration times can be much longer, which leads to improved signal-to-noise performance. Furthermore, unlike in whiskbroom sensors, there is no need for a large, continuously-moving scan mirror or for the scan line corrector, eliminating sources of jitter and possible failure modes. The TIRS focal plane consists of three quantum well infrared photodetector (QWIPs) arrays, a technology flown for the first time on Landsat 8. A segmented filter assembly placed directly over the QWIP arrays provides the spectral band pass.

The TIRS instrument continually gathers image data, but these data are recorded and brought to the ground only on command. Typically, TIRS data are acquired simultaneously with OLI images, but occasionally, at night and in some calibration modes, TIRS data are collected alone. The OLI and TIRS datasets are merged onboard, downlinked in a single data stream and processed into a single product. In addition to normal, nadir-pointed viewing, OLI and TIRS data may be collected in off-nadir viewing geometries and in calibration modes, including lunar viewing and flat fielding modes (the so-called side slither mode in which the field of view is rotated by 90 degrees with respect to its normal mode).

Landsat-8 collects and archives the global, synoptic and repetitive OLI and TIRS imagery and electronically distributes data products to the general public on a no-cost basis [1]. The USGS Earth Resources Observation Systems (EROS) Data Center is responsible for the ground system, including the Ground Network Element, the Mission Operations Element and the Data Processing and Archive System (DPAS). The DPAS consists of several subsystems that produce the Level 0 data and associated metadata and generate the Level 1 radiometrically calibrated and orthorectified images of the Earth's surface, which are located with respect to the standard Worldwide Reference System 2 (WRS2) grid [2,3]. It also includes the Image Assessment System (IAS) developed for OLI and TIRS. The IAS operationally monitors, characterizes and updates the calibrations of the two sensors. The processing algorithms were developed by NASA Goddard and USGS calibration and validation teams.

Requirements Overview

TIRS has nearly 1000 requirements, including detailed performance specifications, spacecraft accommodation, reliability testing, environmental testing, and more [4]. Indeed, there are several hundred performance requirements that cover topics, such as noise, spectral uniformity, banding, streaking, specific spatial characteristics of the instrument function and their temporal stability. With the exception of a stray light exceedance, to be discussed below (and in more detail in [5]), all requirements were met, in some cases with minor waivers. In what follows, only the basic spatial, spectral and noise requirements are discussed. More detail is given in the other papers in this issue [6–8].

TIRS has 100-m spatial resolution, not as fine as the ETM+ on Landsat 7 at 60 m, but higher than the TM sensors with their 120-m thermal band resolution. The 100-m resolution reduces the number of cross-track pixels needed, which aided in meeting the pressing schedule and was determined to be sufficient for TIRS's primary applications, which include agricultural irrigation studies. As defined

in [9,10] and shown in Table 1, the two spectral channels, centered near 10.9 and 12 microns, essentially double sample the single thermal band in the heritage TM/ETM+ systems. The two channels were chosen to allow the use of a "split-window" approach (see, e.g., [11] and the references therein) to compensate for the effects of the atmosphere in converting measured at-satellite radiances into surface temperatures.

Table 1. TIRS band definitions and maximum allowed radiance error.

Landsat Channel	Thermal Band	50% Lower Band Edge (µm)	50% Upper Band Edge (µm)	Center Wavelength (µm)	NEdL Maximum Allowed Radiance Error W/(m^2 sr µm)
10	1	10.6	11.2	10.9	0.059 (0.4 K at 300 K)
11	2	11.5	12.5	12	0.049 (0.4 K at 300 K)

To produce the 185-km swath width of TIRS, 1850 pixels are required for each row in each channel. At a ground speed of 7 km/s, it requires approximately 0.014 s to move 100 m, and 70 frames are taken in each second for each channel. TIRS uses a 3.49-millisecond integration time, and the resultant 25-m image motion, when convolved with the instrument spatial function, does not excessively broaden the spatial resolution. This integration time was chosen to give maximum signal-to-noise performance, while still not saturating at the required high temperature target limit of 360 K. The 10.9-micron channel saturates for target temperatures of about 400 K, while the 12-micron channel saturates at about 370 K. Twelve-bit digitization is used to produce precise temperature measurements over the required range of 240 to 360 K. Pre-launch measurements and in-flight results have shown that temperatures of 180 K (or even less) may be measured with a high signal-to-noise ratio.

Figure 1, taken from [12], shows a comparison of the TIRS spectral bandwidths with those of previous Landsat thermal channels.

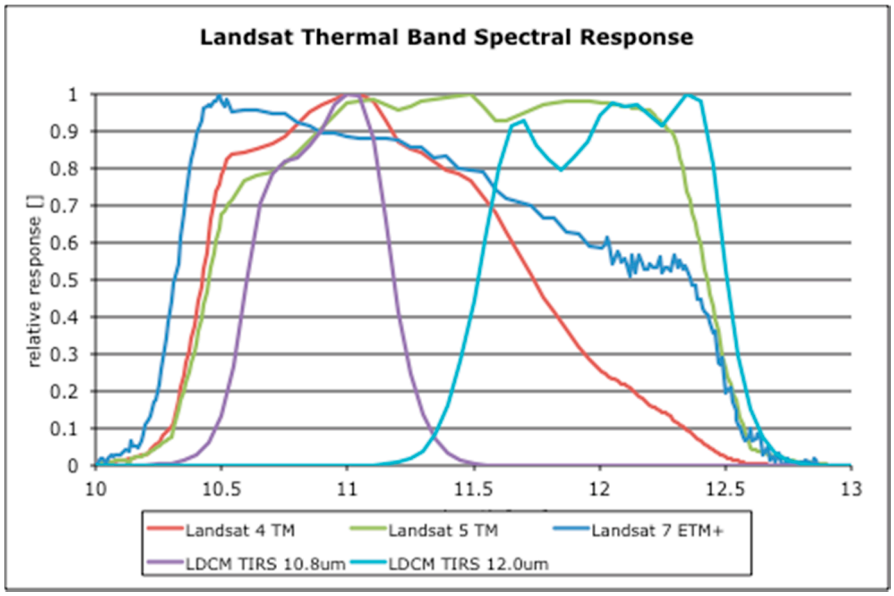

Figure 1. Comparison of the relative spectral response of the Landsat 8/LDCM TIRS thermal channels with those of previous Landsat instruments. The TIRS channels span the same spectral region as the previous versions.

2. Design Overview

Structurally, the TIRS consists of the sensor unit, including the telescope assembly, focal plane assembly (FPA) and focal plane electronics (FPE), two-stage cryocooler, blackbody calibrator, scene select mechanism (SSM), Earth shield, radiators and heat pipes, and two electronics boxes, the main electronics box (MEB) and the cryocooler electronics (CCE). The MEB provides command, telemetry and image data interfaces to the spacecraft, provides power to and controls all functions of the instrument, controls the thermal zones on the instrument (except the cryocooler) and commands the cryocooler electronics. The CCE provides power to the cryocooler and controls its operations and temperature. The FPE provides power and clocking to the three QWIP arrays, and it digitizes the image data. Once every observational period (up to 43 minutes long), the SSM rotates the field of view (FOV) from the ground to the blackbody calibrator and to deep space and then back to the ground. This allows any variation in the instrument thermal background radiance to be removed from the measured radiance and provides regular verification of the calibration response. Figure 2 shows a schematic of the TIRS instrument with the main components identified, and Figure 3 shows a drawing of the TIRS and OLI on the spacecraft next to a picture of the spacecraft prior to launch. To meet its 3.25-year operational lifetime requirement, TIRS employs selective redundancy based on engineering best judgment and validated by analyzing fault trees and performing a failure mode effects analysis (FMEA). In particular, the FPE and SSM have redundant A and B sides, as do some of the other functions of the MEB.

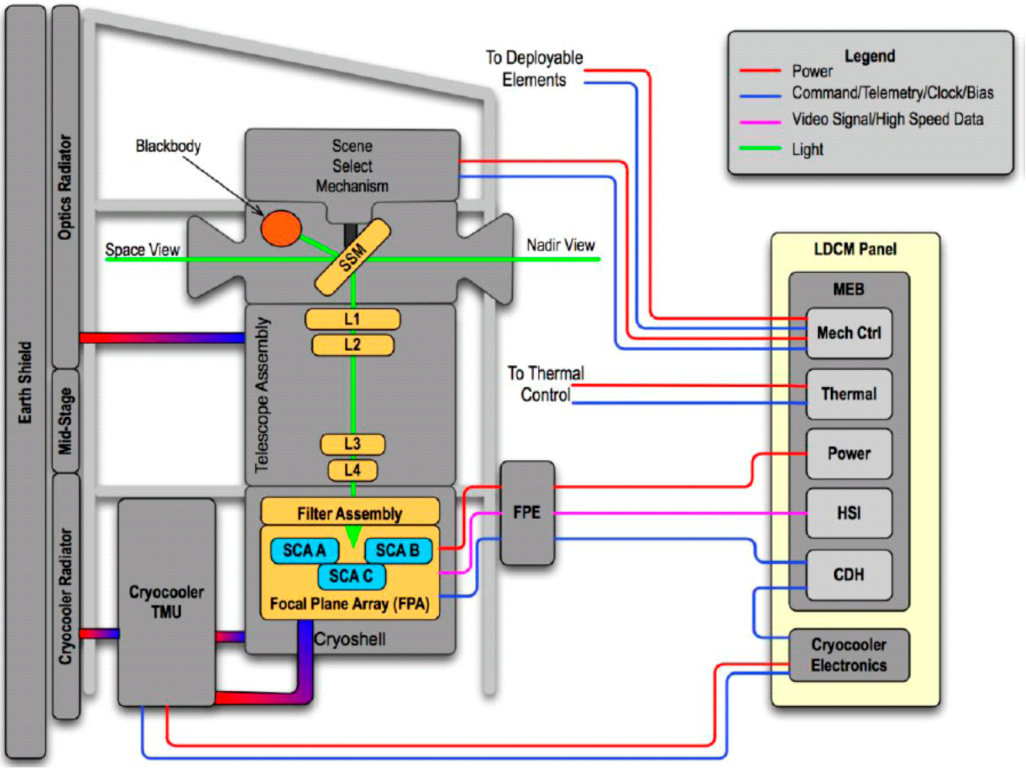

Figure 2. Block diagram showing the interfaces among the major parts of TIRS, including the light paths. SCA A, SCA B and SCA C , the three QWIP sensor chip assemblies (SCA); TMU, thermal-mechanical unit; HSI, high speed interface; L1–L4, the four lens elements; CDH, command and data handling. The other acronyms are defined in the text above.

The f/1.64, 178-mm focal length TIRS telescope uses a temperature-stabilized four-element refractive lens assembly, three germanium (Ge) elements and one zinc selenide (ZnSe) element, to produce nearly diffraction-limited images at the focal plane. The lens elements were fabricated by Nu-Tek Precision Optical Corp. of Aberdeen, MD. All but two of the surfaces are spherical, which simplified fabrication. The lenses were assembled at GSFC. To reduce the thermal background, the TIRS optics are cooled to a temperature between 180 and 190 K using a radiative cooler, and the temperature is stabilized to ~0.1 K using heaters controlled by the MEB. The optics temperature directly affects the focus of the lens, because the Ge index of refraction is a strong function of temperature. The 10-degree temperature range of the optics provides a means of adjusting the focus [9,10].

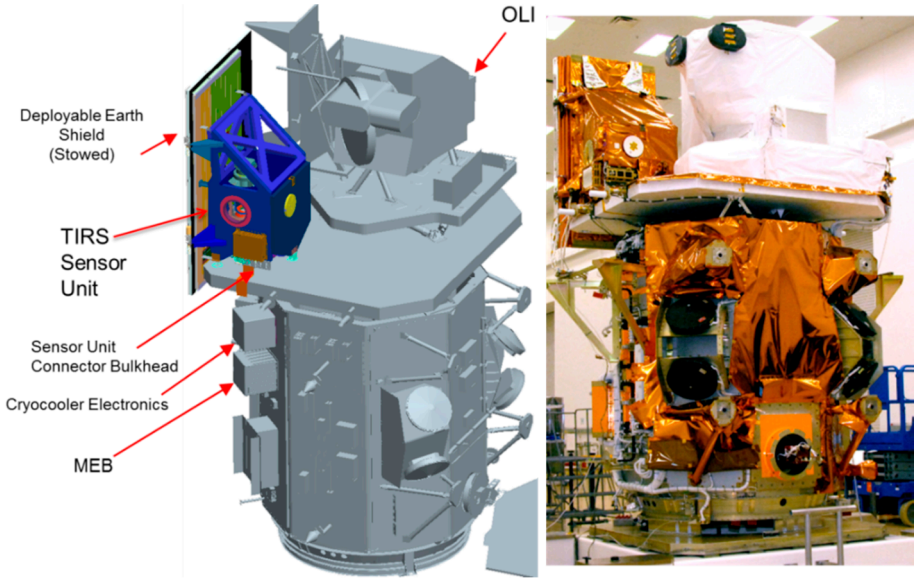

Figure 3. Drawing showing the location of various TIRS components on the spacecraft (**left**) and a picture of TIRS and OLI on the spacecraft prior to encapsulation (**right**).

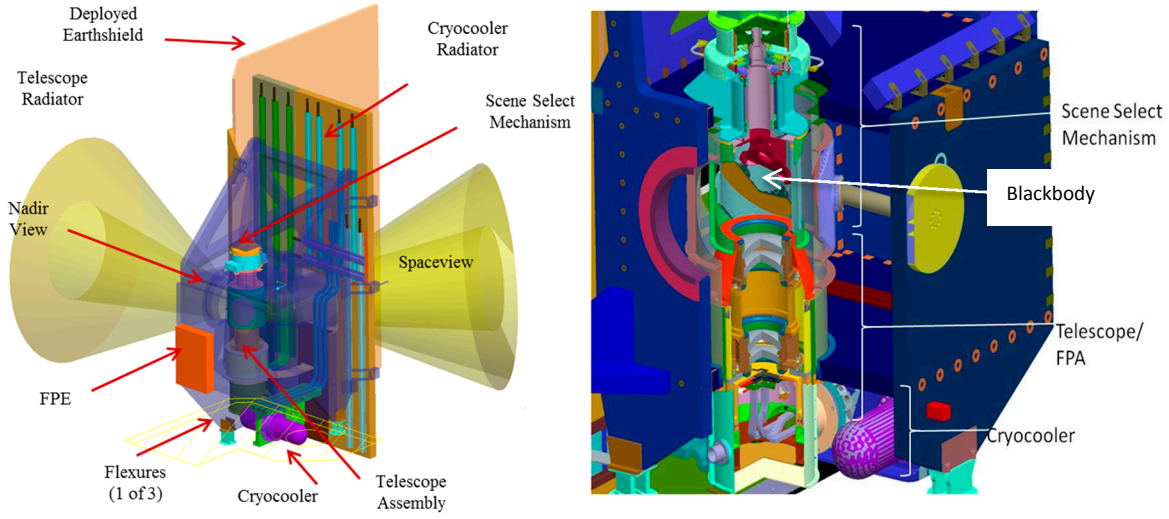

Figure 4. (**Left**) TIRS sensor unit with Earth shield deployed and showing FOVs. (**Right**) Drawing of the optical system, including the SSM, the four lens elements and the focal plane assembly. At the bottom, the cryocooler and the heat straps used to cool the FPA are shown. The blackbody calibration source is shown with its attached radiator.

The focal plane enclosure is cooled to ~100 K, using the first stage of the cryocooler. This further reduces the background thermal level, improving the sensitivity. The focal plane assembly is cooled to about 39 K by the second stage of the two-stage mechanical cryocooler controlled by the CCE. The focal plane temperature is stable to better than 0.05 K, which reduces the noise added by the variability of the dark signal to a very low level. The blackbody calibrator temperature is controlled by the MEB and can be set from 270 to 330 K with an accuracy of 0.1 K. The calibrator was referenced to a NIST traceable calibration standard during ground testing (see Section 3 below). Figure 4 shows a drawing of the TIRS sensor unit with the various fields of view and a model of the TIRS optical system, including the SSM, the four lens elements and the focal plane assembly.

The radiators required to cool the optics and to dump the heat generated by the cryocooler are protected from heating by the Earth by an Earth shield that was deployed soon after launch.

2.1. Focal Plane

The TIRS focal plane uses three 512-pixel by 640-pixel QWIP arrays arranged in a staggered configuration to provide the 1850 cross-track pixels required to cover the 185 km FOV at 100-m resolution. The 25 μm × 25 μm pixels have an IFOV of 141 μradians. Two spectral filters mounted 300 μm above each QWIP produce the spectral shapes shown in Figure 1. The filters were fabricated by Materion Barr Precision Optics and Thin Film Coatings using an ion-assisted deposition process. Figure 5 shows pictures of the focal plane, both before and after the filters are installed.

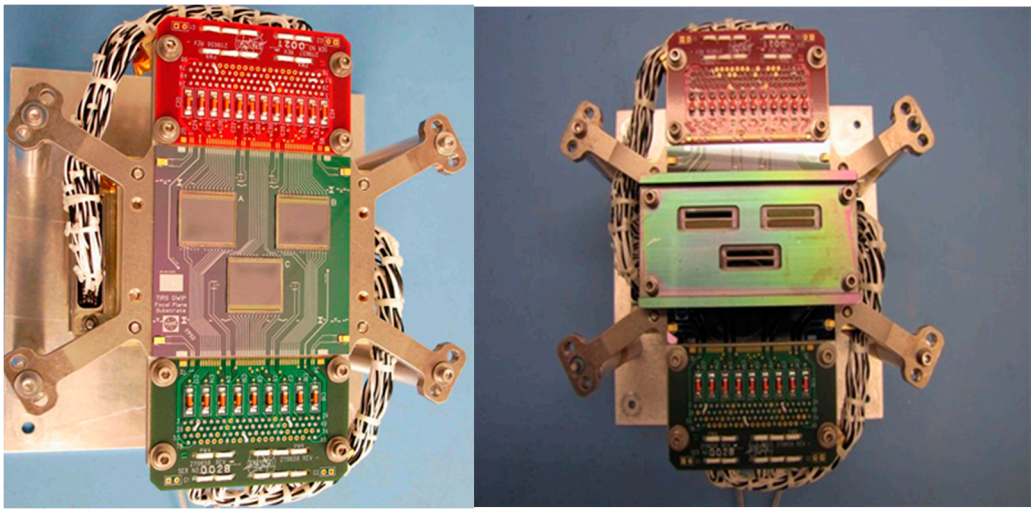

Figure 5. The TIRS flight focal plane with the three QWIP arrays exposed (**left**) and the focal plane with the filter assembly installed (**right**). The six filter segments (two over each array) are clearly visible on the right. The filter assembly is coated on both the top and the bottom with a "black mirror" coating that is less than 5% reflective over the roughly 9–14-μm spectral range over which the QWIPs are active. The coating, which appears greenish in the photo below, limits scattering into the active area of the array.

The QWIP design and fabrication process was a collaborative effort among GSFC, The U.S. Army Research Laboratory (USARL, Adelphi, MD, USA) and QmagiQ (Nashua, NH, USA). All three entities worked on modelling and defining the superlattice growth recipe. The thickness of the gallium

arsenide (GaAs) quantum wells and the aluminum gallium arsenide (AlGaAs) barrier layers and the concentration of aluminum in the AlGaAs primarily determine the band structure in the wells and, hence, the spectral response of the detector material [13,14]. This design was provided to a fabrication house, which deposited 20 alternating layers of GaAs quantum wells and AlGaAs barriers using molecular beam epitaxy (MBE). The resulting detector wafers were sent to QmagiQ, which processed the wafers into arrays up to the point of indium bump fabrication using photolithography, reactive ion etching and vacuum deposition processes. This included etching a periodic structure into the surface of each pixel to form a scattering grating. Each QWIP array was then completed by hybridizing the detector layer to a read-out integrated circuit (ROIC) using an indium bump bonding process. The ROIC contains the integrated electronics that detect the photo-generated electrons and converts the electrons into a voltage. This voltage is proportional to the number of detected photons. Indigo ISC9803 ROICs were used. The hybridization was done at GSFC, where the wafers were diced, most of the substrate was removed and the remaining two-micron layer was polished; the indium bumps were defined and deposited on both the detector layers and the ROICs; the bonding was accomplished, and the epoxy underfill was applied.

The QWIP/ROIC hybrid was then bonded to a custom-developed silicon substrate that contains metal traces. The QWIP hybrids were wire bonded to the traces on the silicon substrate, and this subassembly was attached to an invar baseplate. Also mounted on the baseplate were two printed circuit (PC) boards located at either end of the silicon substrate. Wire bonds connected the silicon substrate traces to these PC "daughter" boards. Connectors on these daughter boards provided the interface between the QWIP hybrids and the FPE.

Because the QWIP detector layer fabrication process is well controlled, the pixels have a very uniform spectral response across each array. Similarly, the pixel response is very stable over time, and there are very few unresponsive or "bad" pixels. These characteristics make the QWIPs excellent sensors in high flux applications, where relatively low quantum efficiency (<1% in the case of TIRS) is not a problem, but where accurate and stable radiometric performance is required.

Figure 6 shows a schematic of the TIRS focal plane with the 36-row un-vignetted active areas under the filters shown. The areas of the hybrids not directly under the filters are shielded from illumination. The filters are wider than the QWIP arrays to reduce scattering from the filter holder edges into the active areas of the arrays. In each of the 70 samples produced per second, six rows are read out from each array: two illuminated rows from the un-vignetted region under each filter (four rows altogether) and two dark rows from an area on the hybrid that is far removed from the filters. The pixels from the illuminated rows in each channel in each hybrid are projected onto the Worldwide Reference System-2 grid. Should a detector fail in a pushbroom instrument, like TIRS, a complete image column of data would be lost. Capturing two rows from each infrared channel on each hybrid allows the ground processing software to combine the two rows into a single "effective" 1850-pixel row that has no inoperable pixels and covers the entire 185-km swath. The dark pixels are read out to provide a measure of the dark current of the QWIP hybrids. This is done to mitigate the effect of variable dark current on the image data in the unlikely event that the temperature of the focal plane is not controlled to sufficient precision by the CCE. Under normal conditions, the dark pixels are not used in data processing.

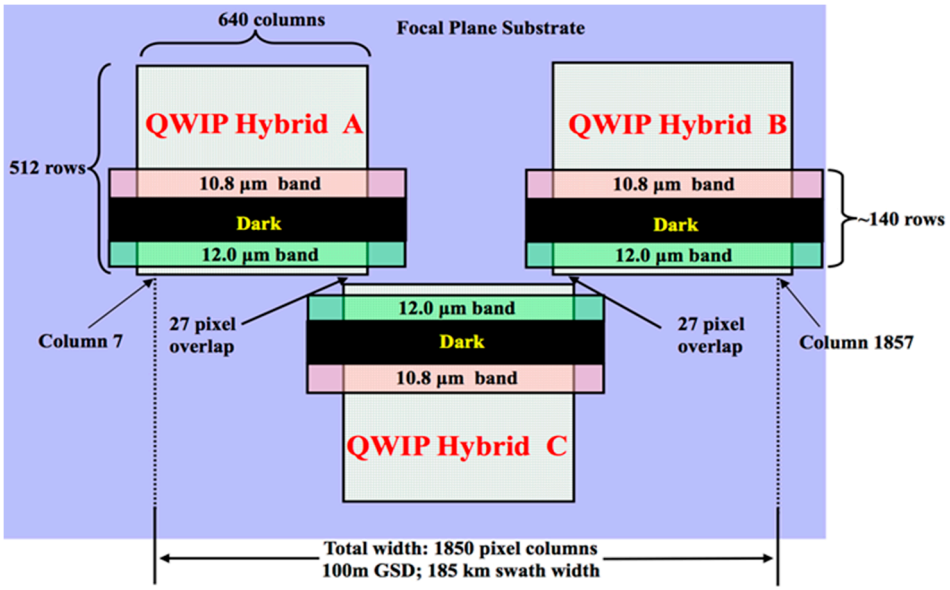

Figure 6. Focal plane layout schematic showing the infrared band locations on the QWIP arrays. The dark area between the filters eliminates scattering between the bands. The first and last seven columns of each array are not used to form the swath. Between that and the fact that there is an overlap area on the ground "seen" by each array, the 1920 total row pixels (3 × 640) are reduced to 1850 pixels.2.2. Electronics

The arrays receive clock signals and biases from the focal plane electronics (FPE). The FPE contains an application-specific integrated circuit (ASIC) chip to gather image data from the QWIP arrays. The System for Image Digitization, Enhancement, Control and Retrieval (SIDECAR) ASIC controls the read pattern on the hybrids and performs analog-to-digital conversion of the image data. The FPE adds header information, formats these data and sends them to the MEB. The MEB packetizes the digitized image data and forwards the packets to the spacecraft communications system to downlink.

The MEB controls the scene mirror position and provides mirror position data to the spacecraft for incorporation into the telemetry. The scene mirror can be positioned with an accuracy better than 10 µradians (3σ) to meet the geodetic requirement that pixel location on the ground be known to 18 m (27 µradians).

The FPE, ASIC and CCE software are loaded from electrically-erasable, programmable, read-only memory (EEPROM), which can be updated from the ground. The MEB uses field-programmable gate arrays (FPGA) for its operations.

3. TIRS Calibration and Pre-Launch Performance

Calibration was performed at the component, subsystem and instrument level throughout the TIRS fabrication process. Comprehensive requirement verification and calibration measurements were made at the instrument level in a thermal vacuum environment prior to shipment of the TIRS for integration with the spacecraft. These latter measurements employed in-chamber calibration equipment with several variable temperature sources for radiometric calibration, which also allowed the spatial and spectral characteristics of the instrument to be characterized by a variety of techniques. In particular, the

calibration equipment included a blackbody cavity source in an Infrared Source Module (IRSM) and a flood source. The latter underwent NIST-traceable laboratory calibration that showed it to be equivalent to a blackbody with an emissivity of 0.992 with an uncertainty of <0.3% at all calibration temperatures required for TIRS [15]. This was the source used to obtain the TIRS radiometric calibration.

The IRSM source is behind a target wheel with apertures ranging in size from a quarter of a pixel to tens of pixels and shapes including circles, squares and extended slits. The output of this source illuminates an off-axis parabola and the aperture can be moved in the X,Y direction in the focal plane of the parabola, as well as in the Z-direction in and out of the parabola's focal plane. The output of the OAP is directed into the aperture of the TIRS instrument by a steering mirror. This optical system allows one to produce target wavefronts equivalent to distant objects at various incidence angles on the TIRS optics. With this functionality, the IRSM and steering mirror allow one to determine the instrument focus, its boresight and the details of the instrumental spatial response. In addition, it allows scattering, streaking, banding, ghosting and distortion characteristics to be investigated and characterized. The calibration equipment structures are cooled to temperatures below 100 K, so that at the TIRS wavelengths, the background illumination produced by them is negligible. Finally, the IRSM module, which is flanked by two sets of "periscope" mirrors, may be moved to place the output of the second "periscope" mirror set at the OAP focal point. In this way, light sources from outside the chamber can be directed through the OAP/steering mirror system to the instrument input aperture. With the output of a grating spectrometer as the external source, this is the configuration used to verify the spectral shape of the two TIRS channels at various places on all three arrays. Figure 7 shows a drawing of the calibration equipment and an example of the light path (in the external source configuration), while Figure 8 shows photographs of it.

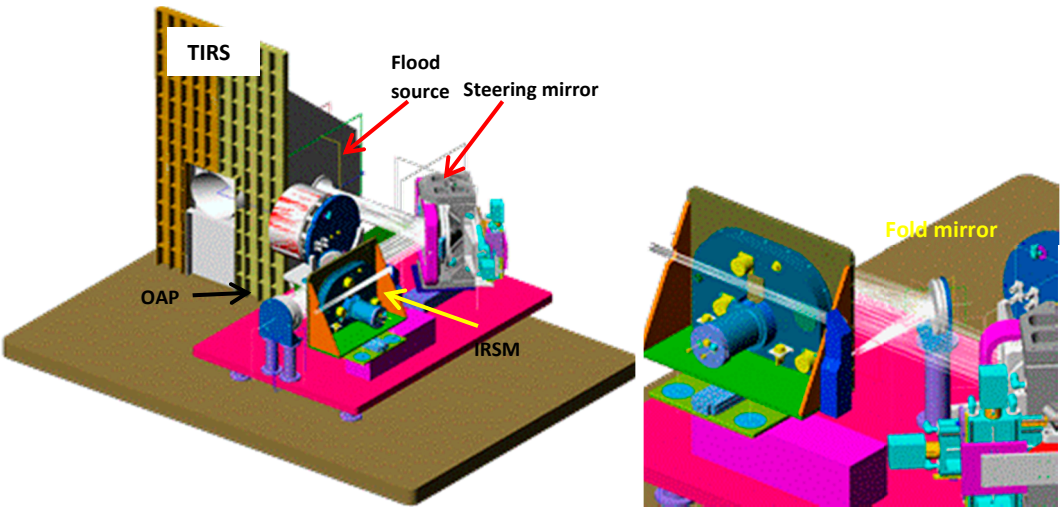

Figure 7. (**Left**) Drawing of the TIRS calibration equipment as placed in the chamber to illuminate TIRS. The various acronyms are defined in the text. In this drawing, which shows the light path for an external source, some of the coverings have been removed for clarity. (**Right**) Detail of the OAP optical system showing the field mirror that directs light from the IRSM to the OAP.

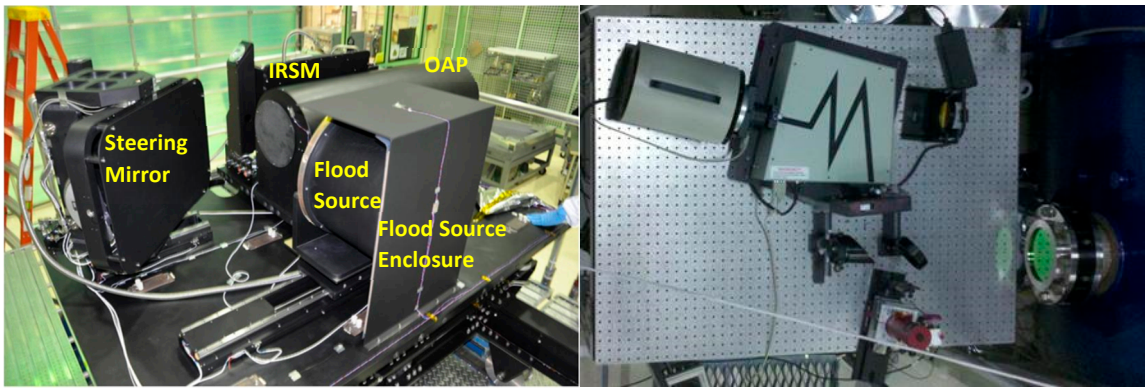

Figure 8. (**Left**) Picture of the TIRS calibration system before it was put into the thermal vacuum test chamber. (**Right**) The grating monochromator system used to verify that the spectral shape of a representative set of pixels was consistent with the product of the component level measurements.

Based on data taken using this system, all performance requirements were met with a few minor exceptions. Waivers were granted for these exceptions, because modeling studies indicated that they would not impact the TIRS data quality. Calibration coefficients were obtained for all pixels in the ~36-row un-vignetted areas of the arrays under the filters. Similarly, 36 rows of dark pixels were obtained for each array. In the normal mode used in-flight, only two rows of pixels under each filter and in the dark areas are obtained. These are the so-called science rows. All pixels in the science rows go through the entire calibration sequence, including georectification. For all locations, either row is fully operational (*i.e.*, all pixels in the row are usable), and the image data for a given channel is based on the first science row of pixels.A high level summary of the overall pre-launch performance is presented below. In summary, the analog signals output by the QWIP pixels, which correspond to the illumination levels, are converted to digital numbers by the ASIC. The illumination levels correspond to the input radiance, which is provided by the calibrated sources. There are non-linearities designed in the QWIP arrays to increase their sensitivity at low light levels. In particular, the output capacitance changes at ~15% of the full well, so that the slope (V/e-) is about four-times higher in the region from 0% to 15% of the full well than it is from 15% to 100% of the full well (see [6] for more details). The first step in the conversion to radiance, therefore, is to linearize the digital output from the arrays for each frame. In this process, all signals are referenced to the slope in the region up to ~10% of the full well. After linearization, the cold background values are subtracted from the values obtained during the nadir calibration observations. The difference represents the calibrated target signal.

Radiometric accuracy: The radiometric calibration was performed using the flood source described above. Required calibrations were obtained at flood source temperatures of 240, 250, 270, 290, 300, 320, 330, 345 and 360 K. At each temperature, the linearized, background-subtracted digital counts generated at each pixel were associated with the calibrated radiance from the flood source. Measurements were made using both the A and B redundant sides of the TIRS electronics over the range of temperatures expected in-flight for the MEB, the FPE and other system components. Each pixel in the active areas of the arrays has a calibration table relating background-subtracted linearized counts to radiance (and brightness temperature) at the flood source temperatures above. The sampling temperatures were chosen such that in no case was there a difference of more than 0.4% between a linear extrapolation of radiances

between two temperatures and an extrapolation using the channel integrated product of τl(λ)* τf(λ)*QE(λ). Here, τf(λ) is the filter transmission as a function of wavelength, τl(λ) is the lens transmission and QE(λ) is the QWIP quantum efficiency. Given this and the better than 0.3% accuracy of the flood source calibration, the requirements of 2% accuracy for temperatures between 260 and 330 K and 4% for the rest of the range from 240 to 360 K are easily met. Final verification of the radiometric accuracy is taking place on-orbit through vicarious calibration methods [16,17].

Noise or NedL: The noise equivalent radiance change is the root mean square (RMS) radiance change over the 30 seconds it takes to obtain a single 185-km × 180-km WRS2 image frame. The required performance is shown in Table 1. Figure 9 shows the results obtained during thermal vacuum testing at 240 K and 360 K, the limits of the required target temperature. As may be seen from this figure, the requirement is easily met by all pixels and with a margin of a factor of five or more for the vast majority. There is also a requirement that the drift over the maximum 44-minute span between deep space looks is <0.7%. This requirement is also met by all pixels with a margin of at least a factor of two.

Figure 9. Noise performance in terms of NEdL and NEdT (noise equivalent temperature change) for the science pixels at 240 K (**top**) and 360 K (**bottom**) measured during thermal vacuum testing. Similar results were found for all flood source temperatures and at all instrument temperature conditions.

Spatial: The TIRS spatial performance was measured during thermal vacuum testing using a variety of IRSM target sources and stepping the steering mirror in sub-pixel steps. The requirements on the instrument spatial performance were levied primarily on the relative edge response (RER, also called the edge response slope) and half edge extent (HEE). These are best defined by reference to Figure 10. As may be seen from this figure, the RER is the ratio of 0.2 to the ground track distance it takes for the instrument response to drop from 60% to 40%. The requirement that RER be greater than 0.007 means this distance must be 28 m or less. The HEE is the ground track distance it takes for the instrument response to drop from 90% to 10%. The requirement is that it takes 150 m or less. Generally, the TIRS RERs were somewhat smaller than required (0.0062 to 0.0068) and the HEEs were somewhat larger (180 to 220 m). However, as the representative measured instrument response function in Figure 10 shows, there is little overshoot or ripple in the TIRS channels, and the TIRS spatial response still meets science measurement needs. Therefore, waivers were granted for the RER and HEE exceedances, which may, or may not, be due to the calibration setup (see [8] for a more complete description of the spatial measurements).

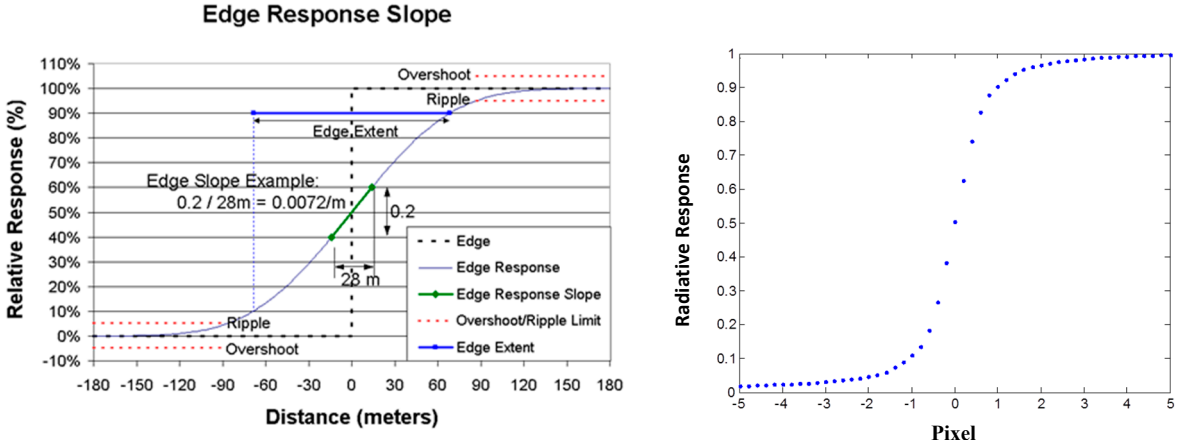

Figure 10. (**Left**) Graphics demonstrating the definition of RER and HEE. (**Right**) Measured instrument response for a representative pixel in the 12-micron channel (TIRS Channel 11). In the graph, each pixel represents 100 m.

Geometric: The geometric (pointing) performance was also measured using the IRSM and steering mirror. The various geometric pointing and stability requirements, as defined in the original requirements matrix, were met with the exception of the measured pointing stability as the instrument temperature was varied over its qualification range. This parameter performed slightly worse than specified in the requirements document. The stability requirement, however, was near the limits of measurement capability, and chamber vibrations and ground support equipment effects contributed to the apparent instability. In [7], a detailed description of the geometric performance using both pre-flight and on-orbit data is presented. There is no measureable on-orbit effect of the temperature-induced pointing instability measured in ground testing.

Spectral: The spectral characteristics of the fully-assembled instrument were measured using the out-of-chamber monochromator. These instrument-level measurements were consistent with the product of the component-level measurements. All spectral requirements are met, although there are some very minor deficiencies in the pixel average response and the in-band spectral variation that

required waivers. These are mitigated by the spectral uniformity of the atmosphere and the surface in the TIRS spectral bands, and no science impact is expected, or seen, in-flight.

Scattering, banding, streaking, ghosting, stray light, *etc*.: These parameters were measured using the IRSM with a combination of targets and beam positions with the steering mirror to simulate both in-field and out-of-field illumination angles. Additionally, the flood source was used in off-axis positions to simulate a large out-of-FOV target (*i.e*., the part of the Earth not in TIRS's 15-degree FOV). All of the performance requirements were met. In some cases, the calibration equipment was not capable of directly illuminating the optics without vignetting. In those cases, an attempt was made to use the SSM to rotate the FOV a few degrees. However, this was not the way the SSM is used in flight, so it was difficult to interpret the results. There were no indications of significant difficulties.

Once on-orbit, however, some anomalous results were obtained when comparing to temperatures of buoys in several bodies of water [16]. That, combined with out-of-field ghosting observed during lunar observations [5], indicated that there was a difficulty caused by the out-of-FOV signal. As it turns out, the total ghosting appears to come from an annulus a few degrees wide, at a radius of ~15 degrees from the boresight. The particular geometry of the ghosting signal seen by a given pixel varies slowly as a function of position in the focal plane. For a uniform field, the ghost signal is only a few percent of the direct signal (about 2% for Channel 10 and 4% for Channel 11). The primary effect of the ghosting is to introduce a positive bias in the measured radiances. When the out-of-FOV radiance is significantly higher than the within-FOV radiance, the effect on brightness temperature can be larger, and the observed radiances can become non-uniform. Detailed optical modeling has indicated that the effect is caused by scattering from a supporting structure above the third lens. The modeling has produced a map of the ghosting source for each pixel. Work is ongoing that indicates a correction algorithm is feasible [5], and a numerical correction algorithm is being implemented. It is important to note that for most regions, the ghosting is not problematic for applications, such as evapotranspiration studies, where local gradients are being assessed and the bias is subtracted out.

4. On-Orbit Calibration Methods

The existing suite of thermal data calibration and validation tools is applied to the TIRS data collected on-orbit, and vicarious calibration continues to play an important role. The IAS has been updated to process pushbroom data, after proving the concept with data from the Earth Observer-1 advanced land imager (ALI), also a pushbroom instrument [18]. Additionally, there are new capabilities on Landsat-8 for calibration and for validation of TIRS. Table 2 lists the types of calibrations that are being used by TIRS on-orbit. Although some of the calibration parameters have changed a bit from their ground-based values [6,7,8,16,17], TIRS performance has been very stable [17] since its initial turn on in orbit.

For normal radiometric calibration, the SSM rotates the FOV from a nadir Earth view to the on-board blackbody calibrator for 60 s and then to deep space for 60 s. This is done twice each orbit, before the first imaging interval and after the last imaging interval (the Landsat 4–7 thermal bands performed similar calibrations twice each data line). TIRS is capable of imaging up to 35 minutes between calibration sequences. The data acquired during these calibration cycles is used during ground processing to correct offsets and gains that may vary over time.

Table 2. TIRS on-orbit calibration data types and their application.

	Detector-to-Detector Relative Calibration	**Long Term Stability (Change Monitoring)**	**Absolute Calibration (Geophysical Parameter Retrieval)**	**Stray Light Effects**
Dark (Deep Space)	X	X	X	
Blackbody	X	X	X	
Vicarious Sites		X	X	X
Side Slither	X			X
	Band-to-Band Registration (within and between sensors)	**Geodetic Accuracy**	**Focus**	**Stray Light Effects**
Geometric Super-sites	X	X		
Focus Check Sites			X	
Lunar Scans				X

The normal calibration sequence described above is replaced on a periodic basis by two other calibration modes: (1) an integration time sweep calibration during the blackbody portion of the normal calibration; and (2) a series of normal calibrations during a blackbody temperature sweep. If required, a stability calibration may be performed in which the normal calibration sequence is repeated every five minutes, for a total of 10-times across 50 minutes.

Since TIRS typically images coincidentally with the OLI, TIRS collects data over the OLI radiometric, geometric and focus check calibration sites, as well as during long land collects and OLI side slither collects. TIRS-driven acquisitions include ocean and night collects. The IAS performs long-term trending, characterization and calibration of the TIRS data and updates the processing parameters as needed.

5. Evapotranspiration Product Comparison between Landsat 7 and Landsat 8

One of the most important products derived from the analysis of a combination of the Landsat visible/NIR and thermal bands is the measure of the evapotranspiration (ET) from regions containing agricultural fields. This product is related to the near-surface water availability and amount of vegetation, and in areas of extensive irrigation, it is related to water usage; a valuable commodity in much of the western U.S. and other arid areas of the world. Figure 11 shows an example of a direct comparison between an evapotranspiration product derived from Landsat 7 and Landsat 8 during the period before Landsat 8 was on the WRS grid when it underflew Landsat 7 on occasion [19]. These data from the Palo Verde, California area (near Blythe) in Path 38/Row 37 were collected on March 29, 2013. The analysis was done using portions of the METRIC (Mapping EvapoTranspiration with high Resolution and Internalized Calibration) ERDAS (Earth Resources Data Analysis System) evapotranspiration code revised for Landsat 8 by the University of Idaho. Because of the ghosting effect noted previously, L8 surface temperatures were artificially biased about 3 K higher than L7 temperatures at 300 K and about 2 K higher at 320 K; however, the METRIC process largely removes bias as part of its methodology [20]. As is evident from this figure, the evapotranspiration maps retrieved using data from the two satellites were very similar, with average differences less than 1%

and an RMS error of 3.5%, which is well within expected uncertainty in ground-based ET measurement [20].

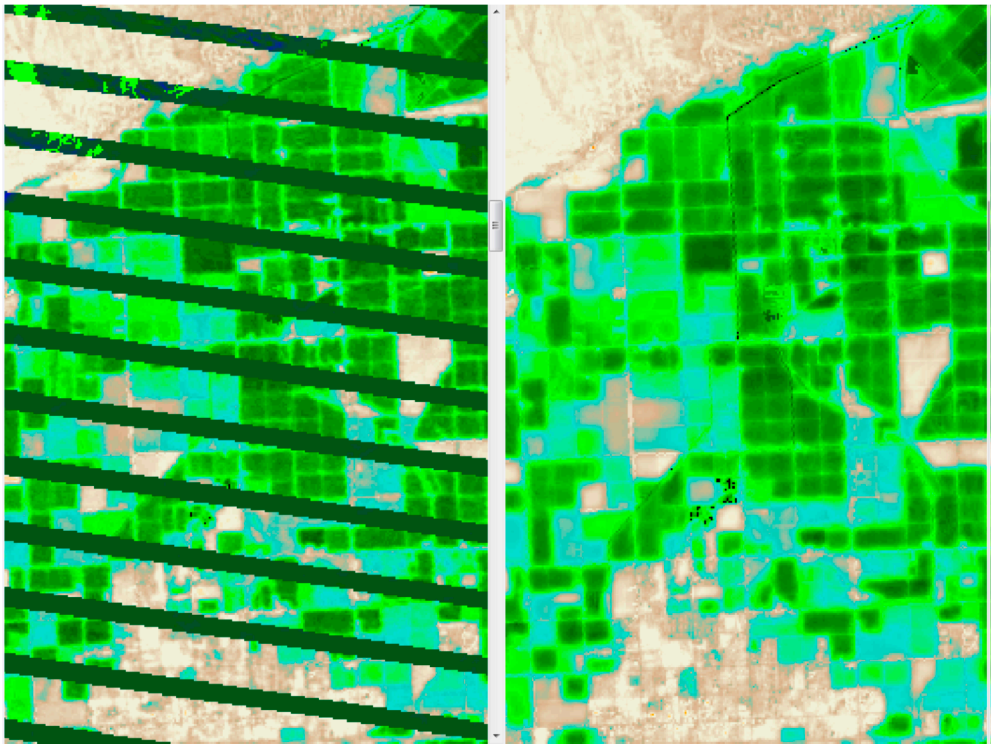

Figure 11. Landsat 7 evapotranspiration product (**left**) compared with that derived from Landsat 8 (**right**). Dark greens indicate higher ET and blues and beiges progressively lower ET. The two maps are quite consistent with each other. Landsat 7 data are sharper, because the Landsat 7 thermal sensor has 60-meter resolution compared to TIRS's 100-m resolution. Data gaps in the Landsat 7 product are due to the scan-line corrector malfunction.

6. Summary

The TIRS instrument, launched as part of the payload of Landsat 8 on February 11, 2013, is a 100-m spatial sampling thermal imager with two channels at about 10.9 and 12 μm. Although the technologies and methodologies used on TIRS are very different from those used on previous Landsat Missions, TIRS still provides thermal data continuity with them. However, its two channels and very high sensitivity provide a new image analysis capability compared to the previous single-channel imagers, such as the ability to do atmospheric correction.

TIRS performance was extensively tested and characterized in a thermal vacuum chamber prior to spacecraft delivery in February of 2012. These ground tests indicated that TIRS would meet its science requirements on-orbit. Since launch, some changes were noted in its performance, and as planned, in-flight changes in calibration coefficients were made to accommodate the changes. In addition, sensitivity to radiance from outside of the field of view was noted. This has a measureable impact on the observed radiances. As of this writing, a numerical correction algorithm for this effect is being implemented. On-orbit TIRS continues to provide very stable outputs.

Acknowledgements

The authors would like to thank all of those who worked on developing TIRS for the Landsat 8 (LDCM) Mission. In particular, they would like to express their thanks to all of those who worked so tirelessly on the TIRS development, analysis, fabrication and test teams. This includes large groups at GSFC, as well as at industrial partners around the country. In addition, TIRS development received active support from numerous parties, including USGS, the LDCM project, the Landsat calibration/validation team, the Landsat science team and NASA HQ. This support was all the more critical given the aggressive schedule required to deliver TIRS on-time and operational for its February, 2013, launch.

Disclaimer: The use of trade-names or identifying commercial suppliers of components or services in this publication does not constitute an endorsement by NASA or the federal government.

Author Contributions

All authors contributed to this manuscript.

Conflicts of Interest

The authors declare no conflict of interest.

References

1. United States Geological Survey. Landsat 8. Available online: http://landsat.usgs.gov/landsat8.php (accessed on 17 July 2014).
2. United States Geological Survey. Earth Explorer. Available online: http://earthexplorer.usgs.gov/ (accessed on 17 July 2014).
3. Bindschadler, R. Landsat coverage of the earth at high latitudes. *Photogramm. Eng. Remote Sens.* **2003**, *69*, 1333–1340.
4. NASA. *Landsat Data Continuity Mission Thermal Infrared Sensor Requirements Document*; Revision F1; NASA Goddard Space Flight Center: Greenbelt, MD, USA, 2012.
5. Montanaro, M.; Gerace, A.; Lunsford, A.; Reuter, D. Stray light artifacts in imagery from the Landsat 8 Thermal Infrared Sensor. *Remote Sens.* **2014**, *6*, 10435–10456.
6. Montanaro, M.; Lunsford, A.; Tesfaye, Z.; Wenny, B.; Reuter, D. Radiometric calibration methodology of the Landsat 8 Thermal Infrared Sensor. *Remote Sens.* **2014**, *6*, 8803–8821.
7. Storey, J.C.; Choate, M.J.; Moe, D. Landsat 8 Thermal Infra-Red Sensor geometric characterization and calibration. *Remote Sens.* **2014**, *6*, 11153–11181.
8. Wenny, B.; Helder, D.L.; Hong, J. Pre- and post-launch spatial quality of the Landsat 8 Thermal Infra-Red Sensor (TIRS). *Remote Sensing* **2014**, in press.
9. Reuter, D.; Richardson, C.; Irons, J.; Allen, R.; Anderson, M.; Budinoff, J.; Casto, G.; Coltharp, C.; Finneran, P.; Forsbacka, B.; *et al*. The thermal infrared sensor on the Landsat Data Continuity Mission. In Proceedings of IEEE International Geoscience and Remote Sensing Symposium (IGARSS), Honolulu, HI, USA, 25–30 July 2010; pp. 754–757, doi:10.1109/IGARSS.2010.5653746.

10. Reuter, D.; Irons, J.; Lunsford, A.; Montanaro, M.; Pellerano, F.; Richardson, C.; Smith, R.; Tesfaye, Z.; Thome, K. The Operational Land Imager (OLI) and the Thermal Infrared Sensor (TIRS) on the Landsat Data Continuity Mission (LDCM). *Proc. SPIE* **2011**, *8048*, doi: 10.1117/12.885963.
11. Kerr, Y.H.; Lagouarde, J.P.; Imbernon, J. Accurate land surface temperature retrieval from AVHRR data with use of an improved split window algorithm. *Remote Sens. Environ.* **1992**, *41*, 197–209.
12. Arvidson, T.J.; Barsi, J.A.; Jhabvala, M.; Reuter, D. Landsat and thermal infrared imaging. In *Thermal Infrared Remote Sensing: Sensors, Methods, Applications*; Kuenzer, C., Dech, S., Eds.; Springer: 2013; Volume 17, pp. 177–196.
13. Jhabvala, M.; Reuter, D.; Choi, K.; Jhabvala, C.; Sundaram, M. QWIP-based thermal infrared sensor for the Landsat Data Continuity Mission. *Infrared Phys. Tech.* **2009**, *52*, 424–429.
14. Jhabvala, M.; Reuter, D.; Choi, K.; Sundaram, M.; Jhabvala, C.; La, A.T.; Waczynski, A.; Bundas, J. The QWIP focal plane assembly for NASA's Landsat Data Continuity Mission. *Proc. SPIE* **2010**, *7660*, doi: 10.1117/12.849305.
15. Space Dynamics Laboratory. *TIRS Flood Source Calibration Report Tech. Rep. SDL/12-863*; Space Dynamics Laboratory: North Logan, UT, USA, 2012.
16. Barsi, J.A.; Schott, J.R.; Hook, S.J.; Raqueno, N.G.; Markham, B.L. TIRS Vicarious Radiometric Calibration. *Remote Sens.* **2014**, *6*, 11607–11626.
17. Montanaro, M.; Levy, R.; Markham, B. On-orbit radiometric performance of the Landsat 8 Thermal Infrared Sensor. *Remote Sens.* **2014**, *6*, 11753–11769.
18. Micijevic, E.; Morfitt, R. Operational calibration and validation of Landsat Data Continuity Mission (LDCM) sensors using the Image Assessment System (IAS). In Proceedings of IEEE International Geoscience and Remote Sensing Symposium (IGARSS), Honolulu, HI, USA, 25–30 July 2010.
19. Trezza, R.; Allen, R.; Kilic, A.; Huntington, J. Revised Preliminary Comparison of Albedo, NDVI, Surface Temperature and Evapotranspiration between Landsat 8 and Landsat 7. Pernal Communication, 2013.
20. Allen, R.G., Tasumi, M.; Trezza, R. Satellite-based energy balance for mapping evapotranspiration with internalized calibration (METRIC)—Model. *ASCE J. Irrig. Drainage Eng.* **2007**, *133*, 380–394